Supplemental Figures

Supplemental Figure 1, Related to Figure 1: Effects of whisking and vM1 suppression on power and coherence of S1 and vM1 LFPs in waking mice

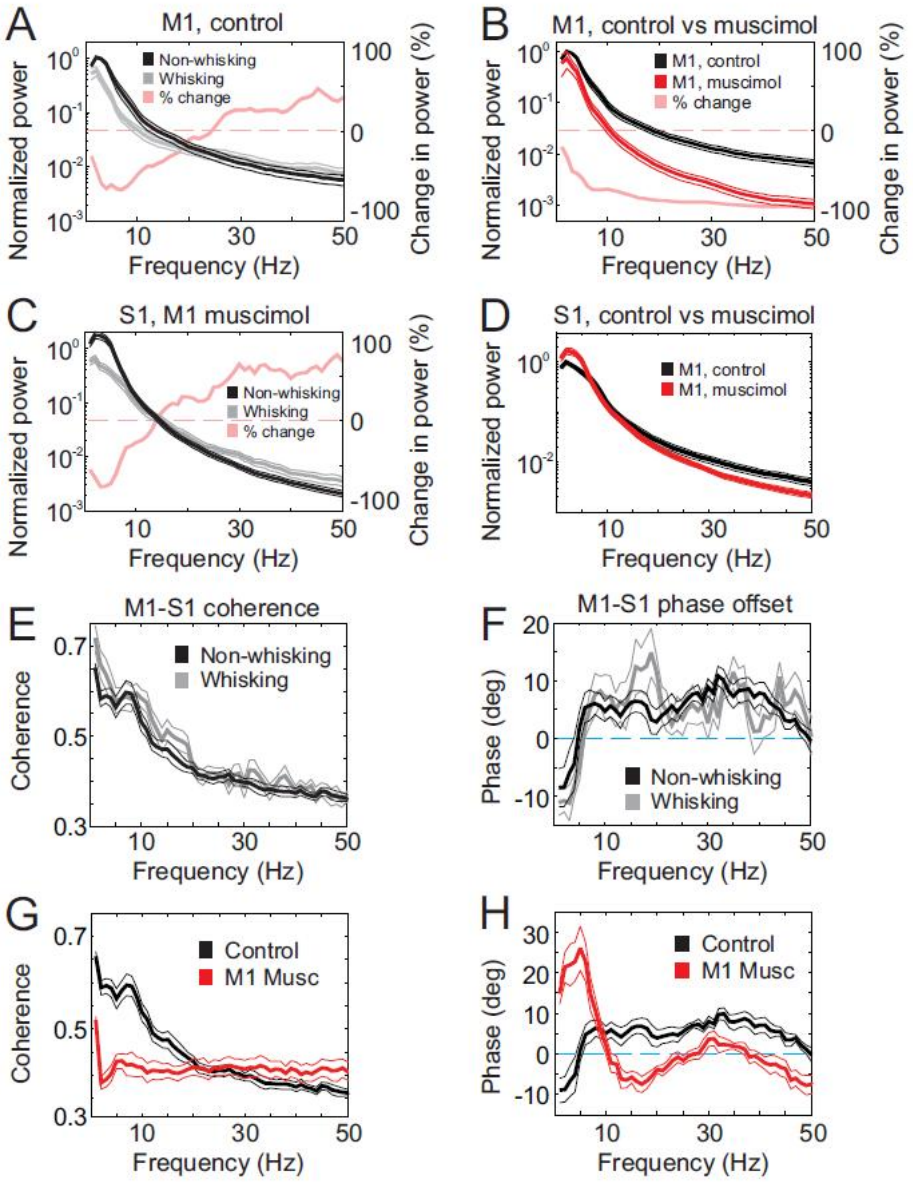

Supplemental Figure 1, Related to Figure 1: Effects of whisking and vM1 suppression on power and coherence of S1 and vM1 LFPs in waking mice

(A-D) Population data, normalized power spectra from S1 and vM1 recordings. Pink solid lines [A-C] are percent changes, referencing scales at the right border of each graph, and pink dashed lines indicate zero change in power. (A) Comparison of vM1 LFP power spectra for whisking (gray) and non-whisking (black) periods. Percent change [100*(whisking-non)/non] demonstrates whisking-evoked vM1 modulation. (B) vM1 LFP power spectra comparing control (black) and vM1 suppression (red) conditions. Muscimol application caused a large decrease in power at all frequencies. (C) S1 LFP power spectra during vM1 suppression, comparing whisking (gray) and non-whisking (black) periods. (D) S1 LFP power spectra comparing control (black) and vM1 suppression (red) conditions. (E, F) Population data of coherence (E) and phase (F) between S1 and vM1, separated into whisking (gray) and non-whisking (black) periods. (G, H) Population data of coherence (G) and phase (H) comparing control (black) and vM1 suppression (red) conditions. vM1 suppression caused a reduction in low frequency coherence (coherence at 2 Hz: 0.59 +/- 0.02; with vM1 suppression: 0.38 +/- 0.01; $p<0.00001$; $n=9$) and reversal of the phase difference (phase difference at 2 Hz: -8.8 +/- 3.2 degrees; with vM1 suppression: 21.5 +/- 3.7 degress; $p<0.001$). This phase reversal may reflect a change in the propagation of slow, spontaneous activity from vM1→ S1 in control conditions to S1 → vM1 during vM1 suppression. Blue lines in (F) and (H) indicate zero phase difference.

Supplemental Figure 2, Related to Figure 3: vM1 stimulation controls and demonstration of graded and rapid effects on S1 activity

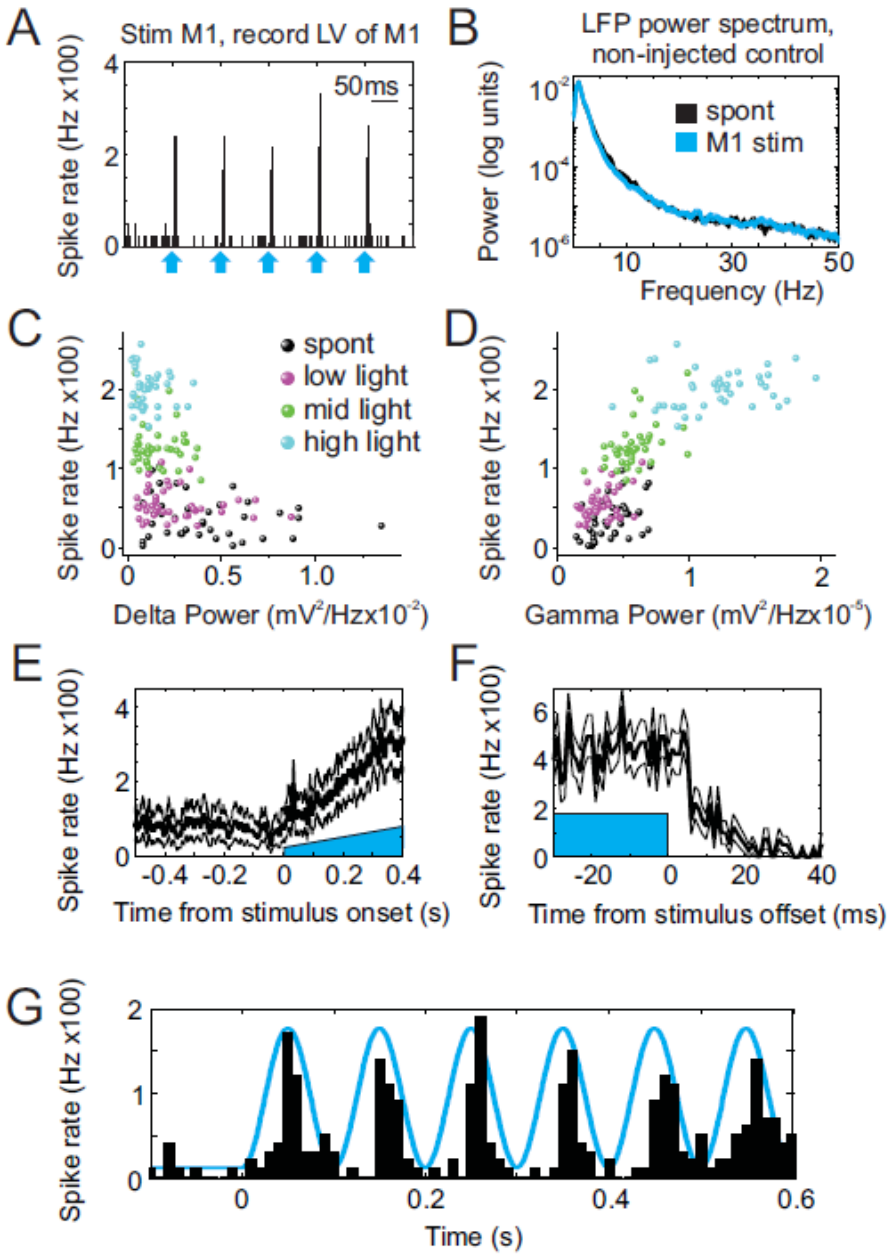

Supplemental Figure 2, Related to Figure 3: vM1 stimulation controls and demonstration of graded and rapid effects on S1 activity

(A) 5 light pulses of 5 ms duration delivered at 10 Hz (blue arrows) was applied at the dural surface above the AAV injection site while recording MUA in LV of vM1. Rapid and transient light-evoked spiking occurred with high temporal precision (Gaussian fit of spike times, full width at half maximum 4.4+/-0.5 ms). (B) S1 LFP power spectra from a non-AAV injected mouse during spontaneous activity (black) and in response to prolonged vM1 stimulation (blue). Light stimulation alone (without ChR2 expression) did not affect S1 activity. (C,D) Single trial data from one experiment, showing relationships between S1 multiunit spike rate and LFP delta power (C) or gamma power (D) in response to multiple vM1 stimulation intensities. Increased S1 spiking with vM1 stimulation was associated exclusively with large reductions in S1 LFP delta power, compared to spontaneous (spont) activity. In contrast, robust increases in gamma power were associated with large increases in spiking. (E-G) Rapid changes in S1 activity driven by vM1 stimulation. (E,F) Shown are average S1 MUA histograms from one experiment, expanded around the onset (E) and offset (F) of light stimulation (blue). MUA is shown at 10 ms (E) and 1 ms (F) bin resolution. (G) Average S1 MUA histogram (10 ms bins) in response to 10 Hz sinusoidal vM1 stimulation (blue). Note that the S1 MUA faithfully followed the oscillatory stimulus, with a lag of approximately 10 ms (depending on stimulus strength and cycle number; n=3).

Supplemental Figure 3, Related to Figure 5: Anatomical and functional analyses of the laminar distribution of vM1 axonal targets in S1

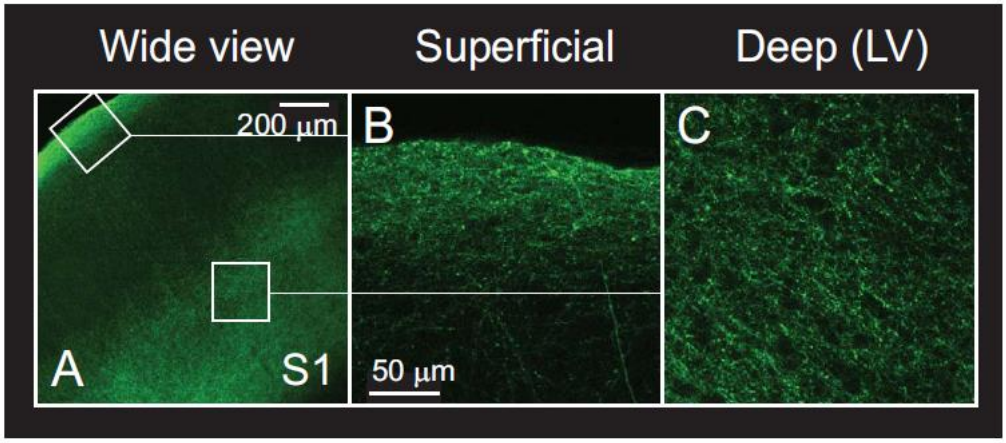

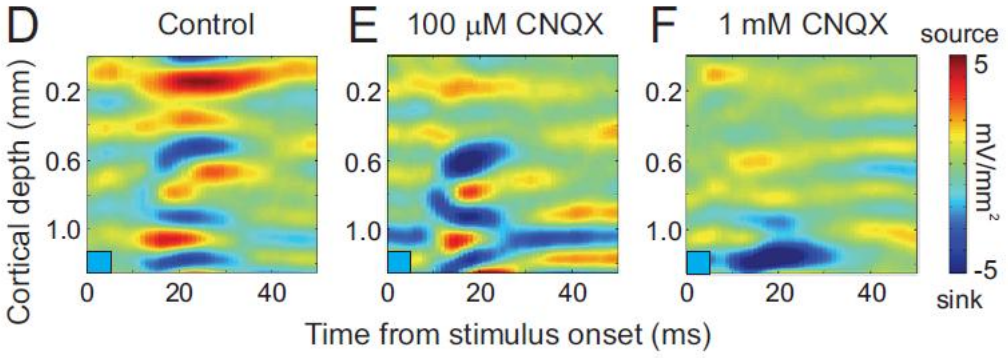

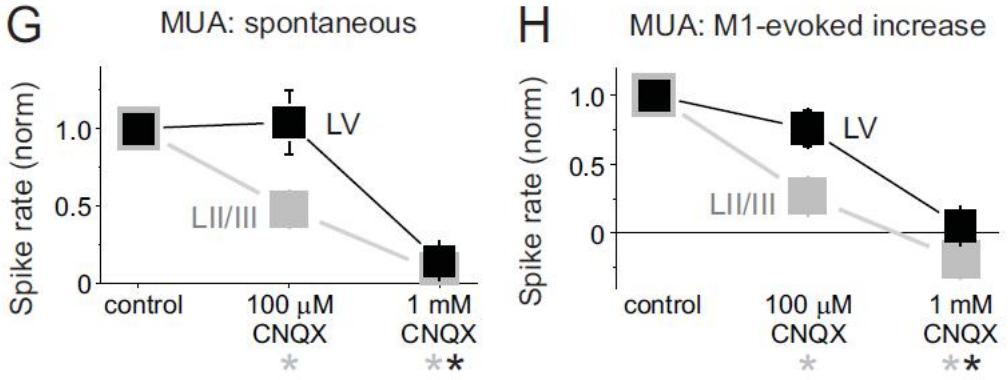

Supplemental Figure 3, Related to Figure 5: Anatomical and functional analyses of the laminar distribution of vM1 axonal targets in S1

(A-C) Images of endogenous fluorescence in S1 four weeks after injection of AAV-ChR2-venus into layer V of vM1. (A) High densities of axons and putative boutons were observed in layer I (B) and layers V/VI (C) of S1. Cell body labeling, from retrograde ChR2-venus expression, was never observed in S1. Scale bar in [B] refers to panels (B, C). (D-F) CSD plots of S1 responses to brief (5 ms) vM1 stimuli (boxes in bottom left corner), in the presence of increasing concentrations of surface applied CNQX. Note the suppression of vM1-evoked dipoles in superficial (E) and superficial and deep (F) layers of S1. (G) Spontaneous MUA from layer II/III (gray) and layer V (black) recordings. 100 μM CNQX significantly reduced spiking in superficial layers, whereas 1 mM CNQX reduced spiking in superficial and deep layers. (H) MUA responses to prolonged vM1 stimulation, normalized to control. Spontaneous firing rates were subtracted to isolate vM1-evoked activity. 100 μM CNQX significantly reduced layer II/III responses to prolonged vM1 stimulation, but not layer V responses. 1 mM CNQX abolished responses from both populations.

Supplemental Figure 4, Related to Figure 6: Effects of thalamic suppression on S1 spontaneous activity and vM1 stimulation responses

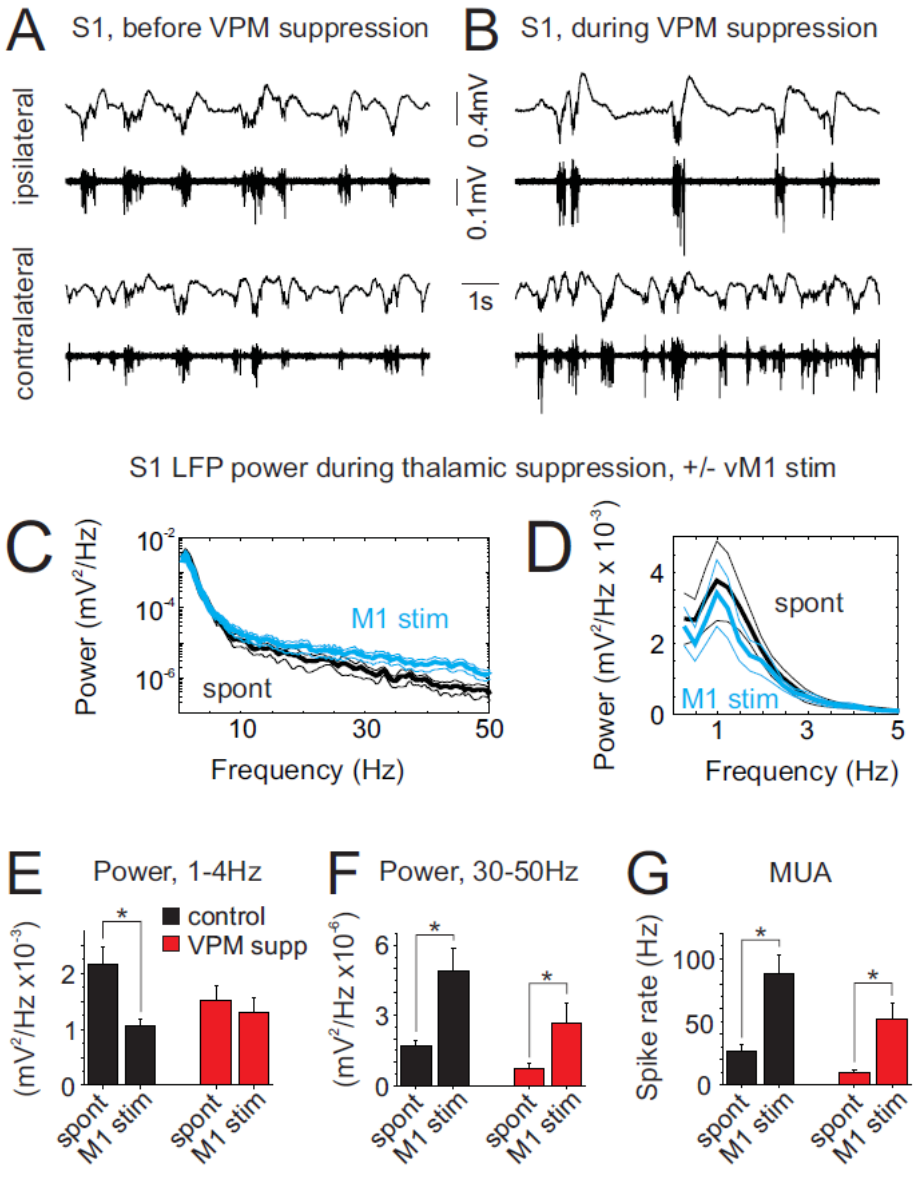

Supplemental Figure 4, Related to Figure 6: Effects of thalamic suppression on S1 spontaneous activity and vM1 stimulation responses

(A) Bilateral S1 signals (LFP and MUA), recorded in anesthetized mice under control conditions. (B) Recordings from the same sites, during unilateral thalamic suppression by focal muscimol injection. Note the reduction in frequency of spontaneous Up-states during thalamic suppression ipsilateral (top) to the thalamic suppression. (C,D) Population average S1 LFP power spectra during thalamic suppression for spontaneous periods (black) and in response to vM1 stimulation (blue). (C) A semi-log plot, revealing vM1-evoked increases in power at higher frequencies. (D) A linear plot, focusing on power at low frequencies. (E-G) Population data, quantifying vM1-evoked changes in S1 delta power (E), gamma power (F) and MUA (G) for control (black) and thalamic suppression (red) conditions. Thalamic suppression caused a decrease in spontaneous S1 LFP delta power, due to a reduction in the frequency of the slow oscillation to below 1 Hz. vM1 stimulation during thalamic suppression did not further decrease S1 LFP delta power. *, $p<0.05$.

Supplemental Figure 5, Related to Figure 8: Analyses of S1 MUA and LFP responses to complex sensory stimuli

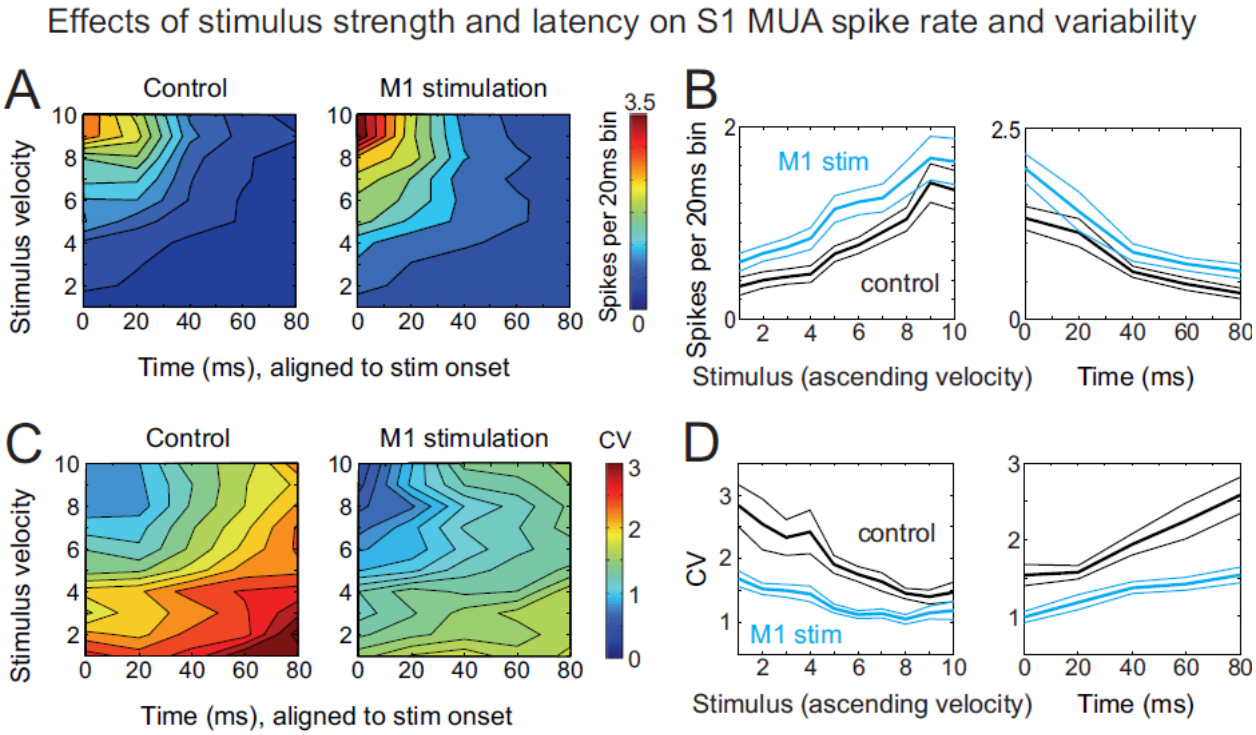

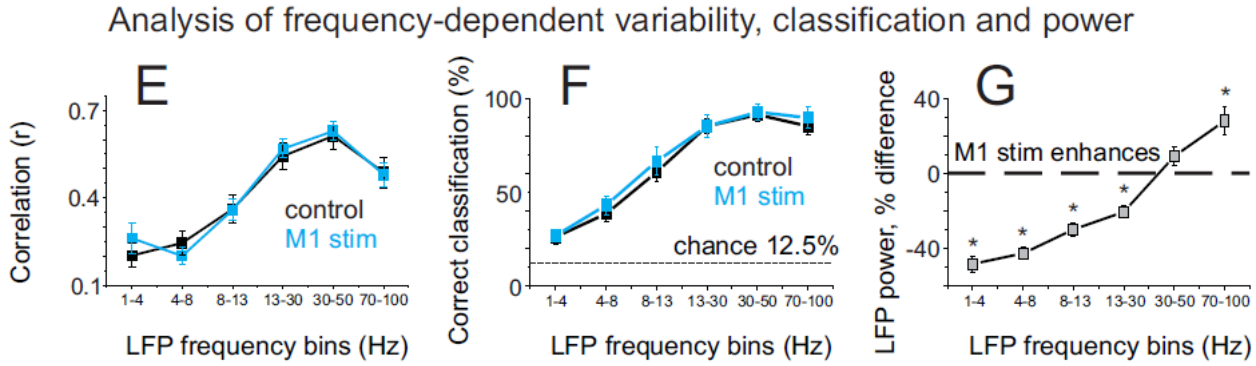

Supplemental Figure 5, Related to Figure 8: Analyses of S1 MUA and LFP responses to complex sensory stimuli

(A-D) Population average, MUA (A,B) and CV (C,D) plotted according to stimulus velocity and latency from stimulus onset. (A) Colormap showing MUA amplitude across both parameters, for control (left) and vM1 stimulation (right) trials. (B) Same data as [A], plotted individually for stimulus strength (left) and latency from stimulus onset (right). Time labels refer to the onset of 20 ms spike histogram bins, with stimulus onset occurring within the first bin. (C,D) Same as [A,B], except for CV amplitude. Note (D, left) that the largest reductions in CV with vM1 stimulation occurred for the weakest stimuli. Similar to this analysis of complex stimuli, we also observed reductions in CV with vM1 stimulation when analyzing only the first stimulus response of each pattern (data not shown). (E-G) Population data, comparing sensory response properties across multiple frequency bands of the S1 LFP. Pair-wise correlation (E) and correct classification (F) of time-domain filtered LFP signals, for control (black) and vM1 stimulation (blue) trials. Trial-by-trial correlation and correct classification increased from delta to gamma frequencies for both control and vM1 stimulation trials. (G) Changes in S1 LFP power during sensory responses, comparing control and vM1 stimulation trials [100*(vM1-control)/control)]. LFP responses from vM1 stimulation trials had reduced power in lower frequencies and increased power in high frequencies. *, $p<0.05$.

Supplemental Experimental Procedures

AAV-mediated ChR2 expression

Male juvenile or adult mice were anesthetized with ketamine and xylazine and a small craniotomy was established over vM1. A glass pipette containing AAV encoding ChR2-venus driven by the CAG promoter was lowered into vM1 (0.8 mm deep) and viral particles were slowly volume injected (0.8 μL over 10 min; Nanoliter 2000). Injected mice were followed for recovery for 3-5 weeks before experimentation.

In vitro preparation

Coronal sections of somatosensory cortex were prepared from mice previously injected with AAV-ChR2-venus in vM1. Mice (aged 50-60 days, approximately 30 days post injection) were deeply anesthetized with sodium pentobarbital (50 mg/kg) and euthanized through decapitation. The brain was rapidly removed and placed in ice-cold (<5°C) cutting solution containing the following (in mM): 110 choline chloride, 2.5 KCl, 7.0 $MgCl_2$, 0.5 $CaCl_2$, 25 $NaHCO_3$, 1.25 NaH_2PO_4, 20 dextrose. Coronal slices, 300 μm thick, were cut on a Leica microslicer in ice-cold cutting solution and transferred to a 35°C incubation chamber containing artificial cerebrospinal fluid (in mM): 126 NaCl, 3.0 KCl, 1 $MgCl_2$, 2 $CaCl_2$, 26 $NaHCO_3$, 1.25 NaH_2PO_4, 10 dextrose, 3 myo-inositol, 2 Na-pyruvate, and 0.4 $_L$-ascorbic acid. Slices were allowed to incubate for at least 1 hour prior to recording. Slices were placed in the recording chamber and imaged with confocal epiflourescence (Yokogawa CSU-22, Solamere Technology, Sapphire 488-20,

Coherent) to identify ChR2-expressing axons in layers I and V/VI of somatosensory cortex.

Histological verification of ChR2 expression

Following in vivo recordings, mice were perfused with 4% paraformaldehyde. Coronal sections were prepared and imaged with a confocal microscope (Zeiss LSM 510).

Pharmacology

AMPA/kainate receptor antagonist 6-cyano-7-nitroquinoxaline-2,3-dione (CNQX) was applied in vivo at the S1 pial surface. For block in superficial layers recordings began 15 minutes after application of 100μM CNQX, whereas for block in deep layers recordings began 30 minutes after additional application of 1 mM CNQX. In a subset of in vitro experiments, picrotoxin (bath, 50-100 μM) was applied to confirm the presence of disynaptic inhibition (n=5).